

# Aspects of advanced catalysis modeling for hypersonic flows

By J. Thoemel<sup>†</sup>, O. Chazot<sup>†</sup> AND P. Barbante<sup>‡</sup>

We report on the recent activities to improve the understanding and the modeling of catalysis of silica exposed to air plasma. Such a combination presents a model for a thermal protection material during an atmospheric entry flight. First, the finite rate catalysis concept is introduced and exemplified using a model available in the literature, then the effect of surface roughness, which leads to a catalysis–diffusion coupling is discussed. The concept of finite rate catalysis and surface diffusion and their interaction is then demonstrated by means of a numerical simulation. It is shown that the catalytic activity is increased by the presence of surface roughness. Finally, the effect of an incomplete energy accommodation is discussed.

---

## 1. Introduction

Vehicles returning from space flight into the atmosphere of a planet experience high wall-heating rates due to the conversion of kinetic and potential energy into heat. Craft that re-enter at moderate speeds between 5 and 8 km/s from orbital or suborbital flights in space station or tourist missions experience moderate heating rates. Consequently, re-usable thermal protection systems are favored due to economic reasons.

The materials used feature high melting temperatures for safety reasons, high emissivities and low catalytic properties in order to lower the heat transfer into the vehicle by re-radiation and a limited chemical gas-surface interaction. Significant efforts have been made in order to quantify the amount of heating, which is due to the latter effect by modeling (Cacciatore *et al.* 1999; Barbato *et al.* 1994) and by experimental techniques (Marschall *et al.* 2006; Schuessler *et al.* 2006). Latest activities are documented to improve the understanding and the modeling of catalysis of thermal protection materials. In Sec. 2, the finite rate catalysis concept is introduced and exemplified using a model available in the literature which is based on surface properties. This has its shortcomings because real surfaces exhibit non ideal properties in particular a surface roughness, which leads to a catalysis–diffusion coupling and is often being ignored. This is discussed first in a 1-D analysis in Sec. 3 and then in a 2-D analysis in Sec. 4. The concept of the coupling of the finite rate catalysis model and surface diffusion model and is then demonstrated by means of computational fluid dynamics simulation in Sec. 5. It is shown that the catalytic activity is increased by the presence of surface roughness. Finally, in Sec. 6, we discuss the effect of an incomplete chemical energy accommodation.

## 2. Finite rate catalysis modeling

The chemical gas surface interaction called catalysis proceeds in three steps:

- diffusion of reactants from the fluid phase to the surface,

<sup>†</sup> Von Karman Institute for Fluid Dynamics, Belgium

<sup>‡</sup> Politecnico di Milano, Italy

- reaction at the surface,
- diffusion of products from the wall to the fluid phase.

Among the reactions possible at the wall are:

- (dissociative) adsorption to the wall,
- desorption from the wall,
- reaction of adsorbed species (Langmuir-Hinshelwood mechanism (LH)),
- reaction of adsorbed species with gas phase species (Eley-Rideal mechanism (ER)).

Each of those reactions takes place with a certain reaction rate, which can be assumed to follow an Arrhenius-type law, i.e., they are temperature dependent (Wintterlin *et al.* 1996; Nasuti *et al.* 1993). In the case of a multi-component plasma flow like air, the possible reaction paths can become very complex due to reactions between different components like NO<sub>x</sub> formation or destruction.

In the hypersonic discipline, one usually simplifies the modeling of catalysis to a recombination coefficient designated  $\gamma$ . This is mainly due to the impossibility of measuring the reaction rates for the different reactions independently. Furthermore, details of the catalysis are of low importance for the design of a thermal protection system and the wall temperature is not accurately known at the instant of time in the design process when computations are carried out. The recombination coefficient models catalysis by a ratio of recombining atoms  $M_{rec}$  over atoms that impinge on a wall  $M^{\downarrow}$ :

$$\gamma = \frac{M_{rec}}{M^{\downarrow}}.$$

Such a ratio can be measured in high enthalpy facilities with relative ease but care must be taken when using such data for computations of atmospheric entry cases that do not thermodynamically coincide with the experimental conditions in which it has been measured.

In contrast one can also quantify catalysis by taking into account every relevant mechanism. Nasuti *et al.* (1996) have proposed a model that takes into account 11 reaction steps. They derive reaction speeds for each reaction from theoretical considerations and surface properties, e.g., the surface migration energy is derived from the Morse potential of the surface. The model includes:

- (a) adsorption of oxygen,
- (b) adsorption of nitrogen,
- (c) ER mechanism of adsorbed oxygen and gas phase oxygen,
- (d) ER mechanism of adsorbed oxygen and gas phase nitrogen,
- (e) ER mechanism of adsorbed nitrogen and gas phase oxygen,
- (f) ER mechanism of adsorbed nitrogen and gas phase nitrogen,
- (g) LH mechanism of adsorbed oxygen,
- (h) LH mechanism of adsorbed nitrogen,
- (i) LH mechanism of adsorbed nitrogen with adsorbed oxygen,
- (j) Desorption of oxygen,
- (k) Desorption of nitrogen.

Furthermore, it assumes a surface inhibition due to OH radicals.

Such a model has the potential to be universally valid, i.e., in any kind of environment. Within the recent research activity, it has been implemented into a module library that can be connected to computational fluid dynamics software. The model by Nasuti *et al.* (1996) is built on surface properties on an atomic level. If applied to CFD, small roughness features existent on actual thermal protection materials (Verant *et al.* 2006) are neglected, which increase significantly the chemical active surface area. This is illus-

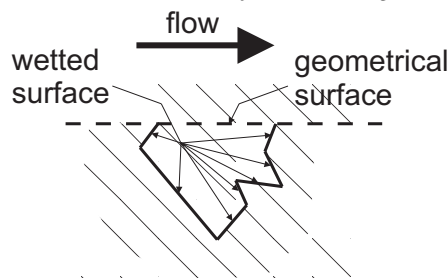


FIGURE 1. Schematic of a surface roughness feature. The actual "wetted" surface on which the catalysis phenomenon takes place can be significantly larger than the geometrical surface seen by an observer.

trated in Fig. 1. Such features stem from the fact that such materials are manufactured using industrial processes.

The roughness caused by the manufacturing decreases in an oxidizing high temperature environment due to an oxide layer forming if the oxygen partial pressure is relatively high and temperatures are moderate. This process is called passive oxidation (Balat *et al.* 1996). If active oxidation occurs, which results in a removal of surface material, the roughness can significantly further increase because the silicon-based materials are usually inhomogeneous and anisotropic (Hald 2003) and consequently material is removed in an inhomogeneous and anisotropic manner. Kim *et al.* (1991) show that the surface roughness has an effect on the catalytic activity of the material, a high surface roughness provides a large actual (wetted) surface available for catalytic recombination reactions. This raises some questions regarding the applicability of the Nasuti model to real, i.e., rough surfaces.

### 3. Catalysis and diffusion in 1-D

The influence of diffusion on catalysis will first be investigated in a 1-D analysis using the recombination coefficient  $\gamma$ . This yields a good understanding of the problem due to the availability of analytical solution even if it neglects important phenomena as multidimensional and rarified effects. This is elaborated in section 4. Though, it can represent the physics in diffusion side-arm reactors (Marschall 2006).

Consider the 1-D steady diffusion equation for atomic species:

$$\frac{d^2 X}{dx^2} = 0, \quad x \in [0, L], \quad (3.1)$$

where  $X$  represents the concentration ( $mol/m^3$ ) and  $x$  is the spatial coordinate. At  $x = 0$ , we assume having the interface to the flow, which acts as a reservoir of species. Thus the boundary condition reads:

$$X(x = 0) = X_0. \quad (3.2)$$

The boundary condition at  $x = L$  accounts for destruction of atomic species by a catalytic reaction. It is derived from the definition of the recombination coefficient:

$$\gamma = \frac{M_{rec}}{M^\downarrow} = \frac{M_{rec}}{X \sqrt{\frac{RT}{2\pi M}}}, \quad (3.3)$$

where  $R$  is the universal gas constant,  $M$  is the molar mass,  $T$  is the gas temperature and  $M_{rec}$  equals the concentration flux. Using Eq. (3.3) and Fick's law, the boundary condition reads:

$$\frac{dX}{dx}|_L = -\frac{1}{D}\gamma_{intrinsic}\sqrt{\frac{RT}{2\pi M}}X(x=L) = -\alpha\frac{X(x=L)}{L}, \quad (3.4)$$

where

$$\alpha = \gamma_{intrinsic}\frac{L}{D}\sqrt{\frac{RT}{2\pi M}}, \quad (3.5)$$

is a Damköhler number based on the surface reactivity and on a diffusion time scale.  $D$  is the diffusion coefficient; the subscript ‘‘intrinsic’’ has been used in order to distinguish recombination coefficients at the surface of a material and recombination coefficients that appear at the interface to the flow which are designated ‘‘apparent’’. This boundary condition is of Robin-type because it relates the gradient of the variable at the boundary to the variable itself. The analytical solution to this problem is:

$$X(x) = \left(-\frac{\alpha}{1+\alpha}\frac{x}{L} + 1\right)X_0. \quad (3.6)$$

The analytical solution provides understanding of the recombination-diffusion competition. First, the concentration at the wall  $x=L$  can be expressed by:

$$X(x=L) = X_0\left(-\frac{\alpha}{1+\alpha} + 1\right). \quad (3.7)$$

One can conclude that the concentration at the catalytic wall tends to the value at the interface of the flow for small Damköhler numbers, i.e., small lengths  $L$  and large diffusion coefficients  $D$ . Secondly, one can define an apparent recombination coefficient, which is the ratio of the concentration flux at the flow interface and the impinging flux of species at the interface:

$$\gamma_{apparent} = \frac{-J|_{left}}{M^\downarrow} = \frac{D(dX/dx)|_{left}}{X_0\sqrt{\frac{RT}{2\pi M}}}. \quad (3.8)$$

After some algebra, one finds:

$$\gamma_{apparent} = \frac{\gamma_{intrinsic}}{\alpha + 1}. \quad (3.9)$$

This expression yields that for small 1-D diffusion lengths and large diffusion coefficients, the apparent recombination coefficient tends to the intrinsic recombination coefficient imposed at the wall. For small diffusion coefficients and large  $L$  the apparent recombination coefficient tends to zero. In this case the catalytic activity is diffusion limited, meaning that less recombination events take place even though the intrinsic recombination coefficient is assumed to be finite and constant and eventually equals one.

#### 4. Catalysis and diffusion in 2-D

The interaction of diffusion and catalysis within the rough surface of a thermal protection material is strongly influenced by 2- or 3-D effects of the surface roughness. In a 1-D situation as shown in Sec. 3, the apparent recombination coefficient only decreases, whereas multi-dimensional effects will increase it. Kim *et al.* (1991) show that the apparent recombination coefficient increases linearly with the surface roughness in a reasonable range of roughness. At extreme roughness, the apparent recombination coefficient levels

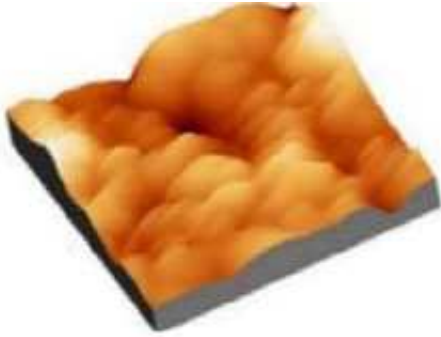


FIGURE 2. Atomic force microscopy photograph of a silicon carbide surface after plasma exposure at the VKI Plasmatron. The size of the slab is  $10 \times 10 \times 1\mu\text{m}$  (Verant *et al.* 2006).

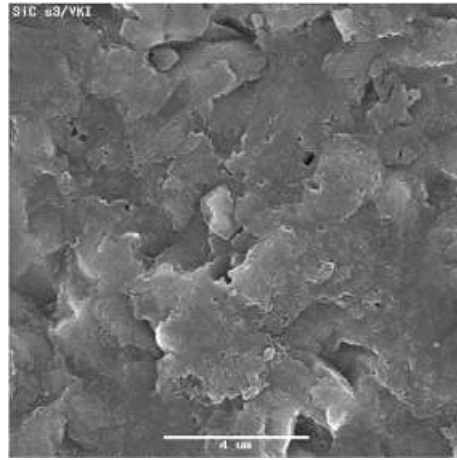


FIGURE 3. Scanning electron microscopy photograph of a silicon carbide surface after plasma exposure at the VKI Plasmatron (Verant *et al.* 2006). The size of the photograph is  $12 \times 12\mu\text{m}$ .

off due to diffusion limitation. Verant *et al.* (2006) have identified the structure of the surface of a TPS after exposure to plasma flow and the researchers discovered that the surface structure is highly complicated with roughness dimensions being of the order of magnitude of  $1\mu\text{m}$

Photographs from this publication are reproduced in Figs. 2 and 3. Such materials are being used, for instance, for the EXPERT re-entry capsule (Muylaert *et al.* 2004; Cipollini *et al.* 2006; Thoemel *et al.* 2007). Based on the trajectory of the EXPERT flight and the dimensions of the surface roughness, a Knudsen number can be defined. It is shown in Fig. 4 together with the expected heating rate. It can be seen that the Knudsen number is fairly low enough for a continuum assumption at the maximum heating during the re-entry. In off-maximum heating conditions the chemical-gas-surface interaction must be treated accounting for rarefaction effects. In order to model the interaction of catalysis and diffusion of real surfaces, we make the following assumptions:

- Due to the small dimensions of the surface roughness, the pressure and temperature are constant and gas phase chemistry and convection effects are negligible within the cavities of the rough surface. Thus, diffusion of species is the dominant phenomenon.
- There is a 2-D rectangular effective cavity that models the diffusion catalysis interaction of more complicated surface roughness cavities.

This enables us to create a simple but sufficient computational model for the effect of surface roughness. It is similarly to the theoretical considerations in Sec. 3's diffusion of species and catalytic surface reactions. In contrast to the analytical solution used in Sec. 3, a 2-D iterative method is employed in order to solve the 2-D diffusion equation:

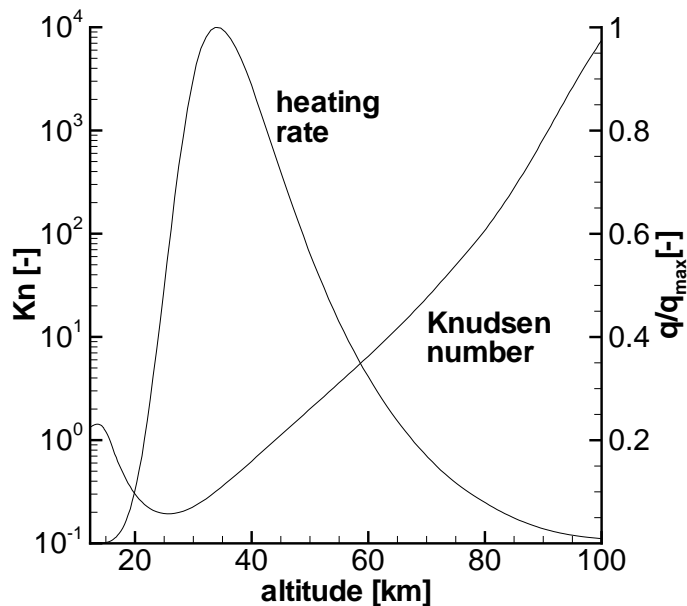


FIGURE 4. Knudsen number and normalized heating rate for the predicted flight trajectory of the EXPERT capsule. The Knudsen number is based on a roughness feature dimension of  $1 \times 10^{-6} m$  and a mean free path (Moore 1972) computed from the expected stagnation pressure based on the DKR formula (Detra *et al.* 1957) and the diameter of the nitrogen molecule (Moore 1972).

$$\frac{\partial X_i}{\partial t} + \frac{\partial J_{i,x}}{\partial x} + \frac{\partial J_{i,y}}{\partial y} = 0,$$

where  $i$  represents the different species in the flow. Analytical solutions exist for the 2-D diffusion equations with catalytic reaction. They are very helpful in gaining understanding of the phenomenon but they are restricted to simple surface reactions of single species (Marschall 2006; Lachaud *et al.* 2007). They cannot be easily utilized when dealing with catalytic reactions of multiple species as described in Sec. 2.

The computational domain is illustrated in Fig. 5. At  $y = 0$ , we assume to have the interface to the flow; the boundary condition reads:

$$X_i = X_{i,flow}$$

The boundary conditions at  $x = L_1$  and  $y = L_2$  reads:

$$J_i = M_{rec},$$

where  $M_{rec}$  can be modeled using the simplified recombination coefficient-type catalysis model derived from Eq. (3.3):

$$M_{rec} = \gamma M^\dagger,$$

or alternatively by the finite rate catalysis model described in Sec. 2. At  $x = 0$  we employ a symmetry boundary conditions:

$$J_i = 0.$$

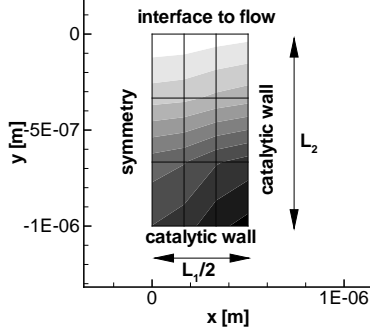


FIGURE 5. The computational domain, the grid, boundary conditions and the solution in terms of concentration of atomic nitrogen. The inlet concentration of N is  $0.1 \times 3.25 \times 10^{-3} \text{ mol/m}^3$  and of  $N_2$  equals  $0.9 \times 3.25 \times 10^{-3} \text{ mol/m}^3$ . A recombination coefficient boundary condition has been used with  $\gamma = 1$ .

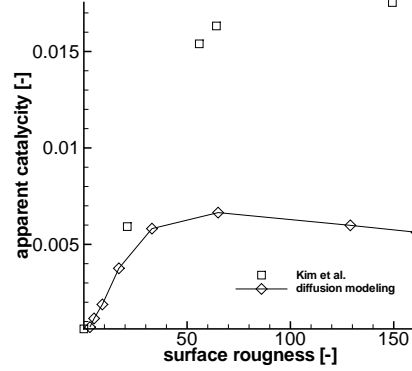


FIGURE 6. Apparent catalytic activity versus surface roughness for a 2-D cavity. The intrinsic catalytic activity is set to  $2.5 \times 10^{-4}$  at the cavity walls, the cavity width is set to  $1 \times 10^{-6} \text{ m}$  and the cavity depth is varied in order to obtain the relevant surface roughness, which is computed as the ratio of the wetted surface to the geometrical surface:  $R = (2 \times L_2 + L_1)/L_1$ .

The diffusion fluxes are computed using the Stefan-Maxwell equations (Giovangigli 1999; Barbante *et al.* 2002). Equation 4 is solved in an explicit way on a coarse, equidistant, orthogonal grid using the cell-center finite volume method:

$$X_{i,j}^{k+1} = X_{i,j}^k + \Delta t \left( \frac{J_{i,j,\text{right}}^k - J_{i,j,\text{left}}^k}{\Delta x} + \frac{J_{i,j,\text{up}}^k - J_{i,j,\text{down}}^k}{\Delta y} \right).$$

The index  $j$  represents the spatial and the index  $k$  the temporal discretization. The apparent recombination coefficient is computed as in Eq. (3.8) averaged over the interface boundary.

The grid and an example solution is shown in Fig. 5. A 2-D concentration field is computed yielding a concentration gradient, thus a mass flux at the flow interface. Kim *et al.* (1991) report on the relation of the intrinsic† to the apparent recombination coefficient of nitrogen plasma on silica glass measured in a diffusion side-arm reactor at low pressure. Such a relation can be reproduced with the diffusion model for a surface cavity length of  $L_1 = 1 \times 10^{-6} \text{ m}$ . The intrinsic recombination coefficient is set to  $2.5 \times 10^{-4}$  and the boundary condition at the interface is set to  $X_N = 0.1 \times 3.25 \times 10^{-3} \text{ mol/m}^3$  and  $X_{N_2} = 0.9 \times 3.25 \times 10^{-3} \text{ mol/m}^3$  as in Kim *et al.* (1991). This is illustrated in Fig. 6.

Estimation of the dimensions of the surface cavity and the roughness parameter poses a difficulty. Only very limited information exists. Kim *et al.* (1991) provide just the latter parameter in their study of silica glass, which is not the material of interest, and artificially roughened material. Verant *et al.* (2006) furnish more details on the surface structures as shown in Figs. 2 and 3 by photographic techniques for a more realistic though generic silicon carbide material. In this study we base our estimations on their findings and consequently we assume a relatively small cavity size. It is to be expected that engineering-type materials (Hald 2003) in in-situ situations particularly if active

† The authors refer to it as the "true" recombination coefficient.

oxidation occurs, possess a very high surface roughness as a consequence of deep surface cavities and the existence of subcavities.

## 5. Results

A simulation of a demonstration case that has been documented in Nasuti *et al.* (1993) has been performed in order to validate the implementation of the Nasuti model and to investigate the effect of surface diffusion on the flow. The VKI code COSMIC (Barbante *et al.* 2006) has been used. It uses the cell-centered finite volume method for hypersonic chemical non-equilibrium flows. Chemical reaction rates for a five-species air ( $N, O, N_2, NO, O_2$ ) have been taken from Park (1993). Thermodynamic properties are computed from statistical dynamics and transport properties from kinetic theory (Bottin *et al.* 1999). The second-order accurate AUSMP scheme has been used for the discretization of the convective fluxes. As in Nasuti *et al.* (1993) a flat plate flow has been computed in a  $0.25\text{m} \times 0.01\text{m}$  domain discretised in  $50 \times 20$  cells.

The results in terms of normalized oxygen mass fraction at the wall is shown in Fig. 7. The VKI solver reproduces well the results of Nasuti *et al.* (1993) in the case of a non-catalytic wall and also in the case of the implementation of their catalysis model within 5% difference. This can be attributed to fact of the use of different transport properties. It can be seen that the use of a catalysis model is reflected by a strong decrease of atomic oxygen, which is consumed by the catalytic reaction.

As a second step the diffusion solver described in Sec. 4 has been used as an interface between the solver COSMIC and the Nasuti catalysis model. Gas phase concentrations at the wall are passed to the diffusion solver, which computes the species distribution inside the cavity using the catalysis model at the sides of the cavity. Mass fluxes are then passed back from the diffusion solver to the flow solver and act as a boundary condition. This procedure is performed for any boundary cell. The dimensions of the effective cavity have been estimated from Verant *et al.* (2006) to be  $(1e - 6m)^2$ . The resulting oxygen distribution at the wall is also shown in Fig. 7. It can be seen that the modeling of the surface roughness increases further the catalytic activity, leading to a further decrease of atomic oxygen at the wall due to its consumption by the wall reaction.

## 6. Incomplete energy accommodation of catalytic reactions

An important aspect of catalysis modeling is to quantify the amount of chemical energy released to the wall by the catalytically formed molecules. The most simple and conservative assumption is to impose that all the chemical energy is transmitted to the wall. There is however experimental evidence (Halpern *et al.* 1978; Balat 2006) that often only a fraction of chemical energy is absorbed by the wall, the remainder is carried away by catalytically formed species that leave the surface in an excited state.

A simple means to characterize this phenomenon is to define a global macroscopic parameter, the chemical energy accommodation (CEA) coefficient  $\beta$  defined as the ratio between the flux of energy effectively entering into the wall,  $q_w$ , and the flux of energy released by wall catalytic chemical reactions,  $q_c$ .  $\beta = 1$  corresponds to full energy accommodation,  $\beta < 1$  to incomplete energy accommodation. Values of  $\beta$  can be obtained by experiments (Halpern *et al.* 1978; Balat 2006) or by theoretical models (Cacciatore *et al.* 1999).

We present now a simple model for the computation of  $\beta$  coefficient; for the sake of

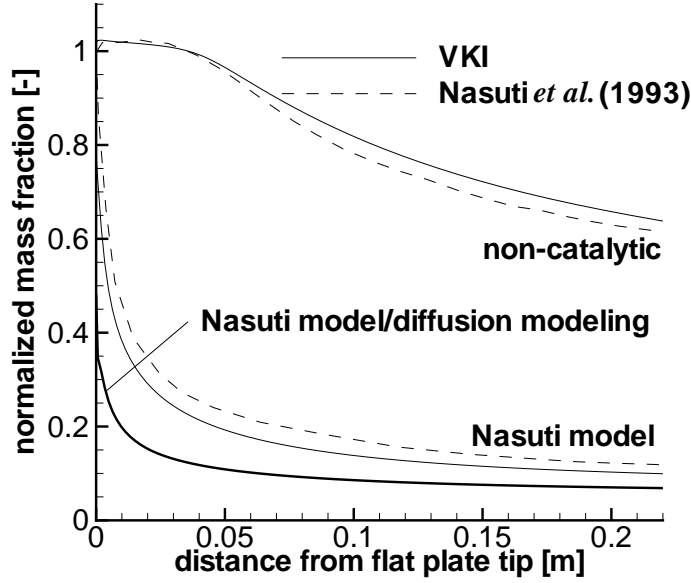


FIGURE 7. Normalized oxygen mass fraction at the wall for chemical non-equilibrium flat plate flow. The inlet conditions and boundary conditions of Nasuti *et al.* (1993) are applied.

simplicity we restrict our attention to a binary mixture made of  $A$  atoms and  $A_2$  binary molecules, but the model is applicable also to a multi-component mixture. The only allowed catalytic reaction is  $A + A \rightarrow A_2$ .

The elementary steps of wall reactions include, as in Sec. 2, adsorption of  $A$  atoms and  $A_2$  molecules, ER and LH reaction  $A + A \rightarrow A_2$ , desorption of  $A$  atoms. The elementary step rates are written as:  $Z_{ad,A}$  for atoms adsorption,  $Z_{ad,A_2}$  for molecules adsorption,  $Z_{ER}$  for Eley-Rideal recombination,  $Z_{LH}$  for LH recombination,  $Z_{de,A}$  for atoms desorption. At every step is associated an energy exchange between the wall and the mixture chemical species that we write as:  $\Delta h_{ad,A}$ ,  $\Delta h_{ad,A_2}$ ,  $\Delta h_{ER}$ ,  $\Delta h_{LH}$ ,  $\Delta h_{de,A}$ .  $\Delta h_R$  is the heat of reaction of  $A + A \rightarrow A_2$  and the following relations can be established:  $\Delta h_{ad,A_2} = 2\Delta h_{ad,A} - \Delta h_R$ ,  $\Delta h_{LH} = \Delta h_R - 2\Delta h_{ad,A}$ ,  $\Delta h_{ER} = \Delta h_R - \Delta h_{ad,A}$ . Partial chemical energy accommodation coefficients for every elementary steps reaction steps are introduced:  $\beta_{ad,A}$ ,  $\beta_{ad,A_2}$ ,  $\beta_{ER}$ ,  $\beta_{LH}$ ,  $\beta_{de,A}$ . The heat flux  $q_c$  writes, for the binary mixture:

$$q_c = \gamma M^\dagger \frac{\Delta h_R}{2} \quad (6.1)$$

whereas heat flux  $q_w$  reads:

$$q_w = \beta_{ad,A} \Delta h_{ad,A} Z_{ad,A} + \beta_{ad,A_2} \Delta h_{ad,A_2} Z_{ad,A_2} + \beta_{ER} \Delta h_{ER} Z_{ER} + \beta_{LH} \Delta h_{LH} Z_{LH} + \beta_{de,A} \Delta h_{de,A} Z_{de,A}. \quad (6.2)$$

The chemical accommodation coefficient  $\beta$  is computed simply as  $\beta = q_w/q_c$ ; when all the partial coefficients are equal to one  $q_w = q_c$  and  $\beta = 1$ . The atom recombination probability  $\gamma$  is computed with the formula:

$$\gamma = (Z_{ER} + 2Z_{LH}) / M^\dagger. \quad (6.3)$$

We apply the model to the determination of CEA coefficient for the catalytic recom-

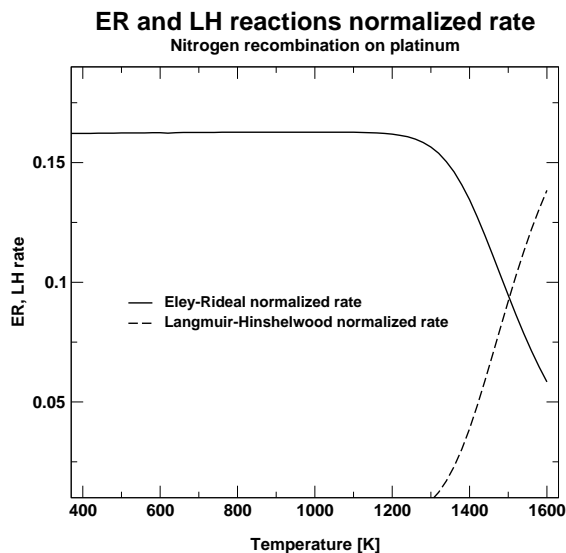


FIGURE 8. ER and LH normalized rate for nitrogen recombination on platinum.

bination of a pure nitrogen mixture of a platinum sample (Halpern *et al.* 1978). The kinetic parameters needed for the computations of the elementary step rates, i.e., the  $Z$  quantities introduced above, are taken from Reggiani (1996). This model predicts that recombination takes place at low temperatures mainly by means of Eley-Rideal reactions, while at higher temperatures LH reactions are more effective. This fact is well-illustrated in Fig. 8; the Eley-Rideal normalized rate is constant between 300 K and 1100 K and sharply decreases above 1200 K, on the opposite the Langmuir-Hinshelwood normalized rate is negligible below 1200 K and strongly increases above it. Model predictions are confirmed by comparison with experimental data as done in Fig. 9: the value of recombination probability  $\gamma$  computed by the theory is in good agreement with the one provided by experiments (Halpern *et al.* 1978). The experiments were carried out for a nitrogen mixtures and the partial pressures the components were 1.33 Pa for  $N$  and 133 Pa for  $N_2$  (Halpern *et al.* 1978).

The prediction of chemical energy accommodation coefficient is more complex; experiments carried out on metals (Halpern *et al.* 1978) and silica surfaces (Balat 2006) show trends of  $\beta$  specific to every material. It is often assumed that Eley-Rideal reactions have a very low partial accommodation coefficient and Langmuir-Hinshelwood reactions an almost complete accommodation. In this case we would expect low values of  $\beta$  for temperatures below 1200 K and an increase of  $\beta$  for temperatures above 1200 K. However Fig. 9 shows that  $\beta$  is around 0.9 for  $T = 500$  K and decreases with temperature. The only possible explanation is that Eley-Rideal reactions have a partial accommodation coefficient that is close to one at ambient temperature and decreases when the temperature increases. The dashed curve, for  $\beta$ , in Fig. 9 is obtained assuming all partial  $\beta$ 's equal to one, except  $\beta_{ER}$ , that is assumed to be equal to one at 300 K and to decrease quadratically with temperature, until it reaches zero at 1600 K. The trend of global  $\beta$  coefficient is correctly duplicated up to a temperature of the order of 1200 K. Above this temperature, theoretical and experimental values diverge and new phenomena, such as partial

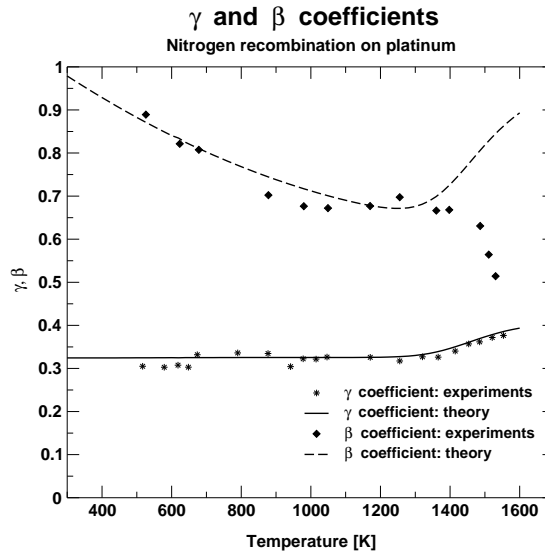


FIGURE 9.  $\gamma$  and  $\beta$  coefficients for nitrogen recombination on platinum.

thermal accommodation of atom adsorption process ( $\beta_{ad,A} < 1$ ), have to be invoked. It is desirable, in future work, to improve the estimation of partial  $\beta$  coefficients, which now is done only by fitting experimental data and is therefore limited to a restricted range of pressure and temperature.

## 7. Summary and discussion

We report first on the effect of surface roughness on the catalytic activity of a thermal protection material. The apparent activity that is seen at the geometrical surface does not reflect the catalysis taking at the surface of the material itself. The roughness of a material increases its activity. This must be taken into account when computations are carried out in the support of the design of a hypersonic vehicle using measured recombination coefficients. The surface roughness may change significantly during flight and might be very different from the roughness of the material that has been used for the measurement of the recombination effect.

The current analysis suggests that further investigations shall be carried out to extend the modeling of the impact of roughness features to flight conditions in which rarified effects are important.

We propose a simple model for the prediction of chemical energy accommodation and compare it to experimental results of nitrogen recombination over metallic surfaces. The agreement is satisfactory, but further work is needed to extend the model to silica materials and to a wider range of temperature and pressure.

### Acknowledgements

The authors thank Dr. Thierry Magin, Dr. Anne Bourdon, Dr. Benjamin Graille and Dr. Jean Lachaud for very helpful discussions. We thank also Prof. Parviz Moin and Prof. Gianluca Iaccarino for their hospitality.

### REFERENCES

- BALAT, M. 1996 Determination of the active-to-passive transition in the oxidation of silicon carbide in standard and microwave-excited air. *Journal of European Ceramic Society* **16(1)**, 55-62.
- BALAT, M. 2006 Interaction of reactive gas flows and ceramics at high temperature. *Experiment, Modeling, and Simulation of Gas-Surface Interactions for Reactive Flows in Hypersonic Flights* NATO AVT-142, VKI Lecture Series
- BARBANTE, P. & SARMA, G. 2002 Computation of nonequilibrium high-temperature axisymmetric boundary-layer flows. *Journal of Thermophysics and Heat Transfer* **16(4)**
- BARBANTE, P. & CHAZOT, O. 2006 Flight extrapolation of plasma wind tunnel stagnation region flowfield. *Journal of Thermophysics and Heat Transfer* **20(3)** 493-498.
- BARBATO, M., GIORDANO, D. & BRUNO, C. 1994 Comparison between finite rate and other catalytic boundary conditions for hypersonic flows. *Sixth AIAA/ASME Joint Thermophysics and Heat Transfer Conference*, June 20-23/ Colorado Springs.
- BOTTIN, B., VANDEN ABEELE, D., CARBONARO, M., DEGREGZ, G. & SARMA, G. 1999 Thermodynamic and transport properties for inductive plasma modeling. *Journal of Thermophysics and Heat Transfer* **13(3)** 343-350.
- CACCIATORE M. & RUTIGLIANO, M. 1999 Eley-Rideal and Langmuir-Hinshelwood recombination coefficients for oxygen on silica surfaces. *Journal of Thermophysics and Heat Transfer* **13(2)**, 195-203.
- CIPOLLINI, F. & MUYLEAERT, J.-M. 2006 European activities on advanced flight measurement techniques for hypersonic space vehicles. *Fifth AIAA Aerodynamic Measurement Technology and Ground Testing Conference*, San Francisco, California
- DETRA, R., KEMP, N. & RIDDELL, F. 1957 Addendum to heat transfer to satellite vehicles reentering the atmosphere. *Jet Propulsion* **27(12)**, 1256-1257.
- GIOVANGIGLI, V., 1999 *Multicomponent flow modeling*, Birkhaeuser, Boston, USA.
- HALD, H. 2003 Operational limits for reusable space transportation systems due to physical boundaries of C/SiC materials. *Aerospace Science and Technology* **7(7)**, 551-559.
- HALPERN, B. & ROSNER D. 1978 Chemical energy accommodation at catalyst surfaces. *Chem. Soc. Far. Trans.* **74**
- KIM, Y. & BOUDART, M. 1991 Recombination of O, N, and H atoms on silica: kinetics and mechanism. *Langmuir* **(7)** 2999-3005.
- LACHAUD, J., BERTRAND, N., VIGNOLES, G., BOURGET, G., REBILLAT, F. & WEISBECKER, P. 2007 A theoretical/experimental approach to the intrinsic oxidation reactivities of C/C composites and of their components. *Carbon* **45** 2768-2776.
- MARSCHALL, J. 2006 Laboratory determination of thermal protection system materials surface catalytic properties. *Experiment, Modeling, and Simulation of Gas-Surface Interactions for Reactive Flows in Hypersonic Flights, NATO AVT-142, VKI Lecture Series*

- MARSCHALL, J., COPELAND, R., HWANG, H. & WRIGHT, M. 2006 Surface catalysis experiments on metal surfaces in oxygen and carbon monoxide mixtures. *Fortyfourth AIAA Aerospace Sciences Meeting and Exhibit*, Reno, Nevada, Jan. 9-12.
- MOORE, W. 1972 *Physical chemistry* (fifth edition), Longman Group, London, Great Britain, 150-157
- MUYLAERT, J.-M., OTTENS, H., WALPOT, L., CIPOLLINI, F., TUMINO, G., CAPORICCI, M., SACCOCCIA, G., BASILE, L., SCHETTINO, A., MOHAMMED, A. & BONNET, J. 2004 Flight measurement technique development for EXPERT, the ESA in flight aerothermodynamic research programme. *Fifty-fifth International Astronautical Congress*, Vancouver Canada, 2004
- NASUTI, F., BARBATO, M. & BRUNO, C. 1993 Material-dependent catalytic recombination modeling for hypersonic flows. AIAA-1993-2840
- NASUTI, F., BARBATO, M. & BRUNO, C. 1996 Material-dependent catalytic recombination modeling for hypersonic flows. *Journal of Thermophysics and Heat Transfer* **10(1)**, 131-136.
- PARK, C. 1993 Review of chemical-kinetics problems of future NASA missions I: earth entries. *Journal of Thermophysics and Heat Transfer* **7(3)**, 385-398.
- REGGIANI, S. & BARBATO, M. 1996 Model for heterogeneous catalysis on metal surfaces with applications to hypersonic flows. AIAA 1996-1902
- SCHUESSLER, M., AUWETER-KURTZ, M., HERDRICH, G. & LEIN, S. 2006 Surface characterization of metallic and ceramic TPS-materials for reusable space vehicles. *Fiftyseventh International Astronautical Congress* Valencia, Spain, Oct. 2-6, 2006.
- THOEMEL, J., TIRTEY, S., FLETCHER, D., CHAZOT, O. & BIRJMOHAN, S. 2007 "Development of an in-flight catalysis experiment within the EXPERT program," *Second European Conference For Aero-Space Sciences*, Brussels, Belgium, July 2007.
- VERANT, J., PERRON, N., GERASIMOVA, O., BALAT-PICHELIN, M., SAKHAROV, V., KOLESNIKOV, A., CHAZOT, O. & OMALY, P. 2006 Microscopic and macroscopic analysis for TPS SiC material under earth and mars reentry conditions. *Fourteenth AIAA/AHI Space Planes and Hypersonic Systems and Technologies Conference*, Canberra, Australia, Nov. 6-9, 2006, AIAA-2006-7947
- WINTTERLIN, J., SCHUSTER, R. & ERTL, G. 1996 Existence of a 'hot' atom mechanism for the dissociation of O<sub>2</sub> on Pt(111). *Physical Review Letters* **77(1)**.